Time-dependent estimates of organ dose and dose equivalent rates for human crews in deep space from the 26 October 2003 solar energetic particle event (Halloween event) using the Earth-Moon-Mars Radiation Environment Module

M. PourArsalan,[1] L. W. Townsend,[1] N. A. Schwadron,[2] K. Kozarev,[2] M. A. Dayeh,[3] and M. I. Desai[3]

Received 21 October 2009; revised 25 March 2010; accepted 30 March 2010; published 19 August 2010.

[1] The Earth-Moon-Mars Radiation Environment Module is being developed for use by a broad spectrum of researchers to predict energetic particle intensities and radiation exposures at any location in deep space. In this work we demonstrate the capabilities of the module for performing analyses of time-dependent exposures from solar energetic particle events at various locations in space by calculating cumulative dose and dose equivalent, and their time rates of change, for the skin and bone marrow of crew members shielded by as much as 10 g/cm^2 of aluminum shielding for the Halloween events of late October 2003.

Citation: PourArsalan, M., L. W. Townsend, N. A. Schwadron, K. Kozarev, M. A. Dayeh, and M. I. Desai (2010), Time-dependent estimates of organ dose and dose equivalent rates for human crews in deep space from the 26 October 2003 solar energetic particle event (Halloween event) using the Earth-Moon-Mars Radiation Environment Module, *Space Weather*, *8*, S00E05, doi:10.1029/2009SW000533.

1. Introduction

[2] Risks to flight crews and instruments from solar energetic particle (SEP) events and Galactic Cosmic Rays (GCR) are a major concern in planning for long-duration manned missions. The central objective of the Earth-Moon-Mars Radiation Environment Module (EMMREM) is to develop a numerical model for completely characterizing the time-dependent radiation environment in the Earth-Moon-Mars and interplanetary space environments. The main challenge in EMMREM is to develop flexible interfaces between the models and observations made in the space science community to assess the radiation environment. We have currently developed a first version of the EMMREM system [*Schwadron et al.*, 2006, 2010].

[3] This estimation and warning ability is currently well supported for different locations on and close to Earth for numerous SEP events. However, estimation of the radiation environment around the Moon, Mars, and other bodies, as well as throughout the solar system is not currently supported for SEP events. Such ability is pivotal for the future development in space, and planned human exploration of the Moon and Mars in the next decades. Propagation of the radiation environments from measurement locations near Earth to other locales in the heliosphere is accomplished using the Energetic Particle Radiation Environment Module (EPREM) module in EMMREM. Details of the EPREM module are presented elsewhere (K. Kozarev et al., Modeling the 2003 Halloween events with EMMREM: Energetic particles in the inner heliosphere, radial gradients, and initial coupling to MHD, submitted to Space Weather, 2010).

[4] With the initial setup of the EMMREM framework in place, we performed realistic simulations with observations from the 26 October 2003 SEP event for module testing and as an example of the module capabilities. Herein we present and discuss the EMMREM predictions for dose rates, dose equivalent rates and accumulated dose and dose equivalent in space throughout the 26 October 2003 event, for observers at Earth, Earth's moon and Mars, for various aluminum shield thicknesses representative of actual space radiation shielding.

[1]Department of Nuclear Engineering, University of Tennessee, Knoxville, Tennessee, USA.
[2]Department of Astronomy, Boston University, Boston, Massachusetts, USA.
[3]Southwest Research Institute, San Antonio, Texas, USA.

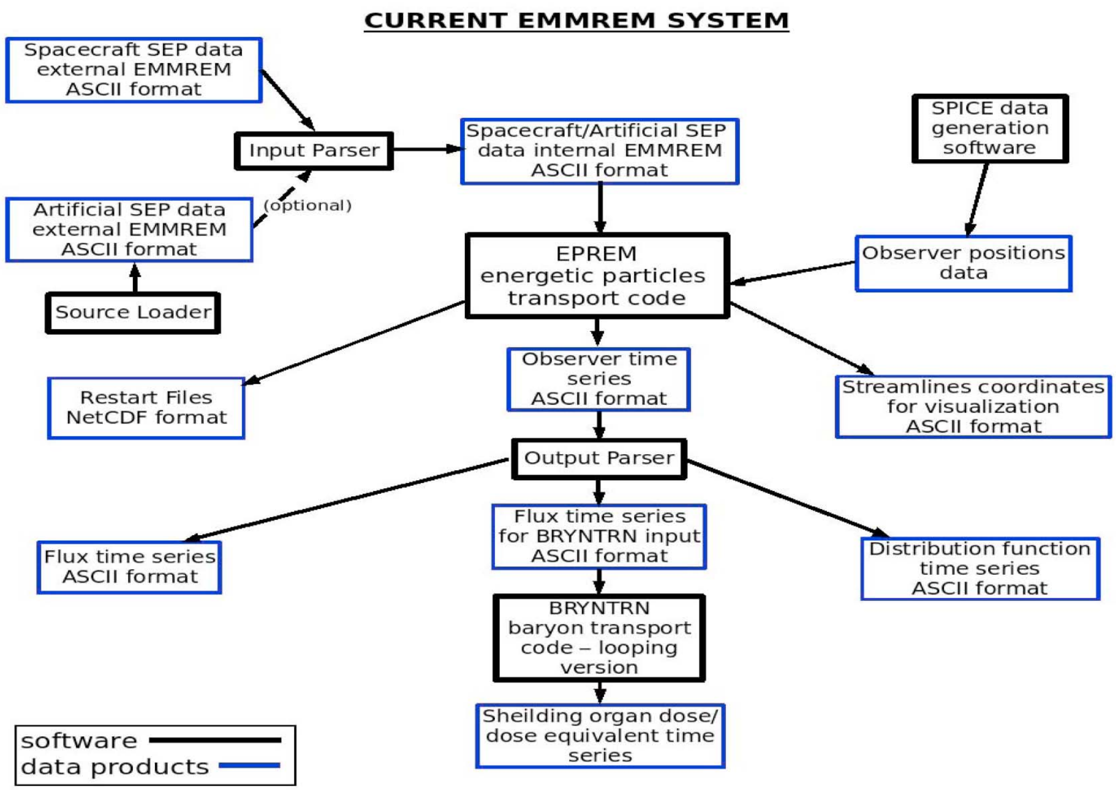

Figure 1. Current EMMREM framework.

[5] Observations at 1 AU were obtained from the Space Environment Monitor (SEM) subsystem on board the Geostationary Operational Environmental Satellite (GOES 11). SEM provides magnetic field, energetic particle, and soft X-ray data. Reported here are the hourly averaged proton intensities measured by the energetic particle sensor (SEM/EPS) at 6 different energy ranges between 4 and 500 MeV. EPS consists of solid state detectors (SSDs) that are wrapped in passive shielding and designed to measure high flux rates without saturation. This design allows high-energy particles from different directions to be counted as if they had entered through the front collimator. Fluxes used here are partially corrected for such effects. Data were obtained from the Space Physics Interactive Data resource (SPIDR: http://spidr.ngdc.noaa.gov/spidr/home.do) of the National Oceanic and Atmospheric Administration (NOAA). The energetic particle flux time series, along with the time series of the Earth, Moon and Mars observers positions are input to EPREM, a 3-D kinetic numerical simulation of the transport of the solar energetic particles throughout the inner heliosphere, in order to estimate the observer time series spectral distributions for various positions. For the work herein, these spectral distributions are transported by EPREM to the vicinity of Mars in order to estimate radiation exposures at that location. The transported flux time series at several energies are then input into the BRYNTRN space radiation transport code [*Wilson et al.*, 1988]. The BRYNTRN code is used to transport incident solar protons and their secondary's through aluminum spacecraft shielding and then through an additional quantity of water simulating human tissue. The BRYNTRN code output contains dose and dose equivalent time series for each of the shielding depths and materials. Details of the EMMREM framework are presented elsewhere in this issue [*Schwadron et al.*, 2010].

[6] In the next section, a brief overview of the EMMREM module framework is presented. This is followed by a discussion of methods used to estimate radiation doses and dose equivalents from the incident space radiation environment. Results of radiation exposure estimates for the 26 October 2003 solar energetic particle (SEP) event (Halloween event) are then presented and discussed as an example of the EMMREM framework capabilities. Finally, the paper concludes with a summary of the work presented.

2. Operational Overview of the Current EMMREM Module

[7] Figure 1 displays a schematic of the current EMMREM operational framework. The blue-bordered rectangles represent input or output data products for the

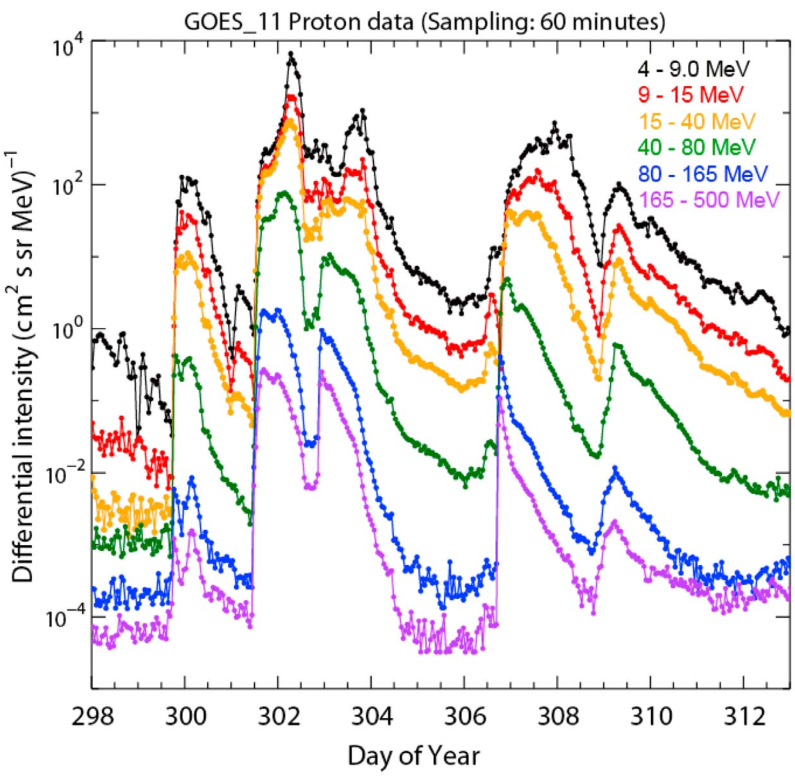

Figure 2. Proton flux versus time for the 26 October 2003 SEP event.

various subsystems. The rectangles with black borders represent the different software products, which are run in series. This whole system is controlled by a number of bash shell and Perl scripts. The EMMREM Module is a UNIX based system. The whole package is run in LINUX OS (UBUNTU V8.04).

[8] The EPREM transport code takes two types of input data: (1) energetic particle flux time series and (2) the positions of various bodies of interest in the simulation in heliospheric inertial coordinates. Major components of the EMMREM System are described below.

[9] 1. The input parser converts the external EMMREM format data (from GOES, ACE, other spacecraft, etc.) into internal EMMREM format data (distribution function time series of SEPs).

[10] 2. The SPICE positions loader is generated by utilizing the CSPICE library of the NASA SPICE Toolkit.

[11] 3. The EPREM submodule is a 3-D kinetic numerical simulation of solar energetic particles transport throughout the inner heliosphere. It is a parallelized code written in C/C++.

[12] 4. EPREM output includes observer time series of distribution function spectra for various positions in the code (ASCII internal EMMREM format).

[13] 5. The output parser converts observer outputs from distribution function time series to flux time series for several energies.

[14] 6. The BRYNTRN transport code uses output parser outputs as inputs [*Hatcher et al.*, 2009]. BRYNTRN is a deterministic transport code written in FORTRAN 77, which is parallelized. The BRYNTRN is used to transport incident solar protons and their secondaries through aluminum spacecraft shielding and then through an additional quantity of water simulating human tissue. The BRYNTRN output contains dose and dose equivalent time series for different shielding depths and materials.

3. Radiation Dose and Dose Equivalent Calculation Methods

[15] The outputs of the output parser for the incident proton spectra at each location for the October 2003 SEP event, shown below in Figure 2, are transported through an aluminum shield and the simulated human geometry using a deterministic, coupled neutron-proton space radiation code, BRYNTRN, developed at NASA Langley Research Center. For this work, the incident proton spectra and their reaction products (neutrons, protons, ^{2}H, ^{3}H, ^{3}He and ^{4}He) are transported through up to 10 g/cm^2 of aluminum and then through an additional 10 g/cm^2 of water which simulates body soft tissue. One g/cm^2 of water is a reasonable substitute for the actual body self-shielding distribution associated with skin and eye exposures, and 10 g/cm^2 is reasonable for the blood

Table 1. Permissible Exposure Limits for Short-Term or Career Noncancer Effects Taken From *NASA* [2007]

Organ	30 Day Limit (cGy-Eq)	1 Year Limit (cGy-Eq)	Career Limit (cGy-Eq)
Lens[a]	100	200	400
Skin	150	300	400
BFO	25	50	NA
Heart[b]	25	50	100
CNS[c]	50	100	150
CNS[c] ($Z \geq 10$)	-	10	25

[a]Lens limits are intended to prevent early (<5 years) severe cataracts (e.g., from a solar particle event).
[b]Heart doses calculated as average over heart muscle and adjacent arteries.
[c]CNS (central nervous system) limits should be calculated at the hippocampus.

forming organs (BFO) [*Bier et al.*, 1998; *Townsend and Zapp*, 1999; *Lin*, 2009]. These organ self-shielding substitutes were selected for use in order to test the ability of the EMMREM framework to carry out real-time calculations, for updated particle flux intervals as small as five minutes, during an actual event. These will be replaced in the future by realistic body organ self-shielding distributions [*Billings and Yucker*, 1973] obtained from actual human geometry models. The transported particle fluxes are converted to dose and dose equivalent using the methods described by *Wilson et al.* [1991]. Absorbed dose or simply dose (symbol D) is the primary physical quantity used in radiation protection. It is defined in International Commission on Radiation Units and Measurements (ICRU) Report 51 [*ICRU*, 1993] as the mean energy imparted by ionizing radiation to matter of mass m. The dose unit is in Joules/kg (gray). The dose needed to achieve a given level of nonacute biological risk (mainly for cancer indication or mortality) is different for different types of radiations. To account for this, dose is multiplied by a unitless constant called the quality factor (Q), which is defined in International Commission on Radiological Protection (ICRP) Report 60 [*ICRP*, 1991], and is a function only of LET in water (a tissue surrogate). The product of dose (D) and quality factor (Q) is called dose equivalent (H). If the dose is in gray (Gy), dose equivalent is in Sievert (Sv). Dose equivalent for a particular organ is not compared to limits. Instead, it is used to compute a quantity called effective dose (E), which is a weighted average of organ dose equivalents over a variety of organs (more than 15). Since the focus of this work is to demonstrate the near real-time capabilities of EMMREM to estimate dose, calculations of effective dose are beyond the scope of the current work. Career limits are given in terms of effective dose, which are cumulative for the entire career or lifetime of the exposed individual.

[16] The results of the simulations are compared with the short-term permissible exposure limits (PELs) used by NASA for human activities in space [*NASA*, 2007]. These limits are shown in Table 1. These exposure limits, which pertain to short-term (e.g., acute) and career noncancer effects are expressed in units of centigray equivalent, which are obtained from the absorbed dose (D) as

$$\mathrm{D(cGy - Eq.) = D(cGy) \times RBE} \quad (1)$$

where the absorbed dose is the average energy absorbed per unit mass in tissue (1 Gy = 1 J/kg), and the RBE (relative biological effectiveness) is a multiplicative factor that should be applied [*National Council on Radiation Protection and Measurements*, 2000] to account for the ability of some radiations to produce more noncancer and acute biological damage than others for the same dose. RBE is defined as

$$RBE = D_X/D \quad (2)$$

where D the dose of radiation of a particular type (protons or alphas for example) necessary to produce some biological end point (e.g., radiation sickness) and D_X is the dose of a reference radiation (usually X-rays or gamma rays) needed to produce that same effect. RBE, as defined by equation (2) is a function not only of LET, but also of particle type, dose rate, dose levels, and the particular biological effect, such as acute radiation syndrome (radiation sickness) or chromosome aberrations, etc., being investigated. For SEP protons an RBE value of 1.5 is assumed, as recommended by the National Council on Radiation Protection and Measurements for proton induced acute exposure responses.

4. Results

[17] Earth, Moon, and Mars observer results for the specified aluminum and water layers are presented. The proton energies for the input solar particle data are from 4 to 500 MeV. Aluminum shielding areal densities, which simulate actual shielding used for manned space missions are 0.3 g/cm^2, nominal spacesuit; 1.0 g/cm^2, thick spacesuit; 5.0 g/cm^2, nominal spacecraft; and 10.0 g/cm^2, SEP storm shelter.

[18] The calculated results presented herein for different observers help us to understand the possible variations in severity of space radiation exposures during the event based on the EPREM results at different locations in the inner heliosphere.

[19] Figures 3, 4, 5, and 6 depict the dose equivalent and dose results for the Earth observer. Since the Moon is very near Earth, the radiation environment for the Earth and the Moon observer is very similar. Therefore estimates of the skin and BFO gray equivalents are essentially identical (differences are much less than 1%). Thus, only results for the Earth observer are presented at 1 AU.

[20] As expected, the predicted rates of skin and BFO dose and dose equivalent for the Earth observer rise and fall in the same pattern as the SEP fluxes as a function of time. The thicker the aluminum shielding, the lower the exposures, also as expected. The accumulated skin and BFO dose and dose equivalent results show increases for the higher exposure rates, and then the expected leveling

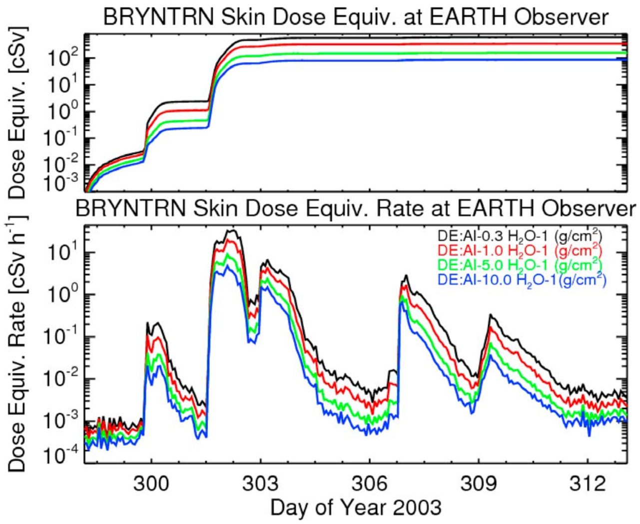

Figure 3. (top) Accumulated skin dose equivalent and (bottom) skin dose equivalent rates near Earth at 1 AU during the 26 October 2003 Halloween events. The aluminum (Al) and water (H_2O) depths in g cm^{-2} are displayed in the legend in the bottom plot.

off trends as the exposure rates decrease. Note that the 30 day skin dose limit is exceeded for aluminum shield areal densities corresponding to a spacesuit on day 302 (29 October) and for nominal spacecraft thicknesses on day 303 (30 October). The BFO dose limits are exceeded for aluminum shield areal densities corresponding to spacesuit thicknesses on day 301 (28 October), and to nominal spacecraft and storm shelter thicknesses on day 302 (29 October). The latter, however, are not large enough to

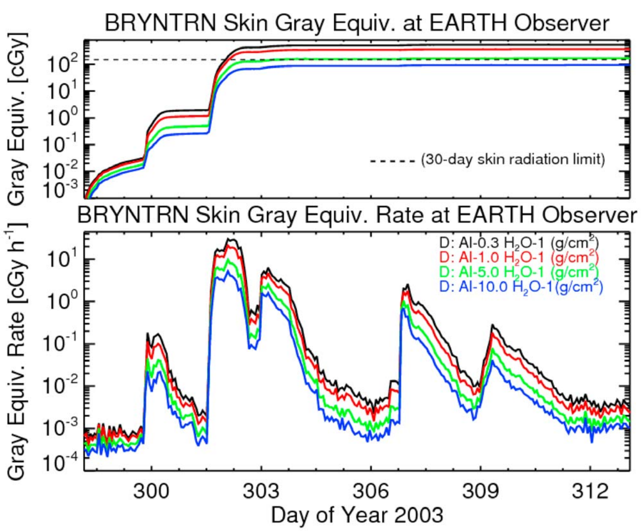

Figure 4. (top) Accumulated skin gray equivalent and (bottom) skin gray equivalent rates near Earth at 1 AU during the 26 October 2003 Halloween events. The aluminum (Al) and water (H_2O) depths in g cm^{-2} are displayed in the legend in the bottom plot. Also displayed are the 30 day skin dose limits (150 cGy equivalent), which are exceeded for the three thinnest aluminum shields.

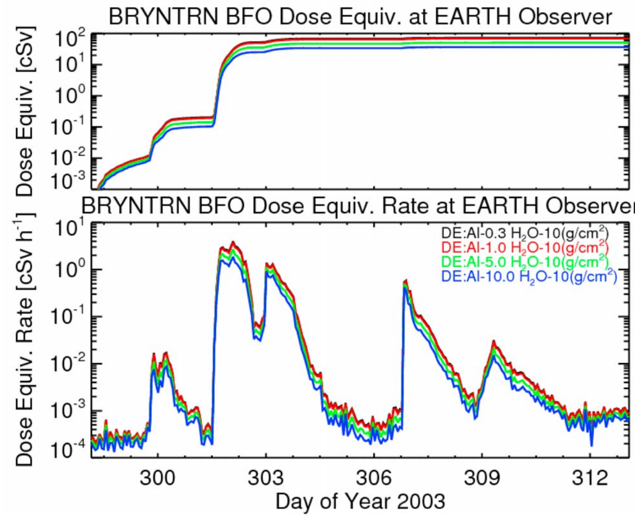

Figure 5. (top) Accumulated BFO dose equivalent and (bottom) BFO dose equivalent rates near Earth at 1 AU during the 26 October 2003 Halloween events. The aluminum (Al) and water (H_2O) depths in g cm^{-2} are displayed in the legend in the bottom plot.

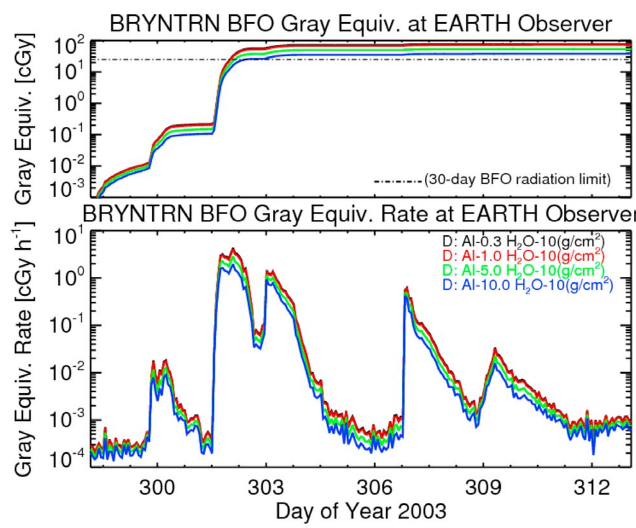

Figure 6. (top) Accumulated BFO gray equivalent and (bottom) BFO gray equivalent rates near Earth at 1 AU during the 26 October 2003 Halloween events. The aluminum (Al) and water (H_2O) depths in g cm^{-2} are displayed in the legend in the bottom plot. Also displayed are the 30 day BFO dose limits (25 cGy equivalent), which are exceeded for all four aluminum shields.

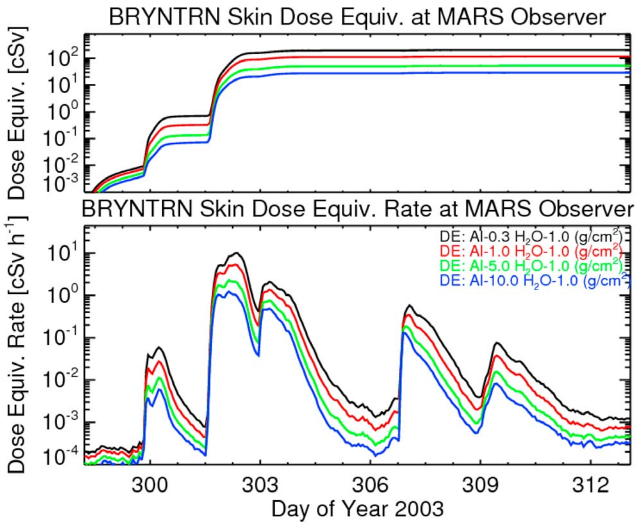

Figure 7. (top) Accumulated skin dose equivalent and (bottom) skin dose equivalent rates near Mars during the 26 October 2003 Halloween events. The aluminum (Al) and water (H_2O) depths in g cm^{-2} are displayed in the legend in the bottom plot.

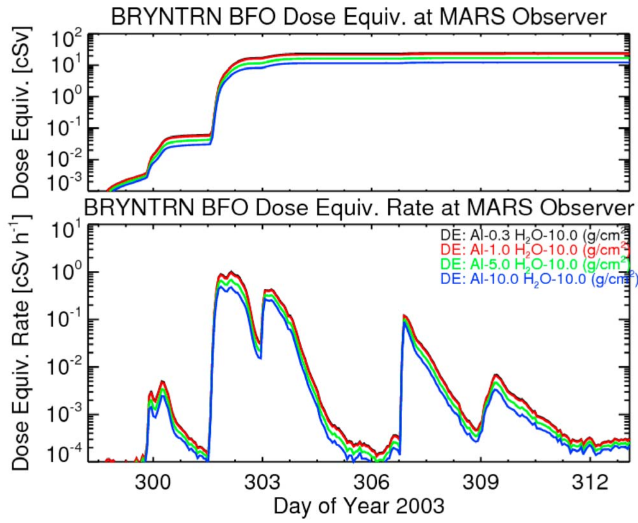

Figure 9. (top) Accumulated BFO dose equivalent and (bottom) BFO dose equivalent rates near Mars during the 26 October 2003 Halloween events. The aluminum (Al) and water (H_2O) depths in g cm^{-2} are displayed in the legend in the bottom plot.

cause any acute radiation syndrome (radiation sickness) effects. Although the dose level for the skin is below its respective limit if the crewmember is inside the SEP storm shelter, the BFO limit is exceeded even if the crewmember is inside a storm shelter. Since there are no dose equivalent limits for individual organs, such as the skin or BFO, similar comparisons for dose equivalent are not made.

[21] Turning our attention to the results for the Mars observer, which are displayed in Figures 7, 8, 9, and 10, note that the 30 day skin dose limit is exceeded for this event at Mars for the spacesuit aluminum shield areal densities on day 303 (30 October). Note also that the 30 day BFO dose limit is exceeded for spacesuit shielding on day 306 (2 November). However, if the crewmember is inside a spacecraft or SEP storm shelter, then no dose limits are exceeded. The dose levels at the Mars observer are lower due to the lower particle fluxes at this location, relative to the fluxes experienced by the Earth and moon observers, who are closer to the sun.

5. Comparison of the Peak Dose Rates and Accumulated Doses of October 2003 Event With August 1972 Event

[22] Estimates of peak dose rates and accumulated doses of protons in the skin and bone marrow, behind various thicknesses of aluminum shielding, for crews on space missions near 1 AU but outside Earth's magnetosphere were previously published for the large SEP event of August 1972 using the coupled neutron-proton radiation transport computer code BRYNTRN [*Parsons and Townsend*, 2000]. Since the proton fluence measurements for this event at high energies are not well characterized or constrained, a similar analysis using EMMREM is not possible. However, we can estimate what the possible doses at Mars might have been for this event by extrapolating the

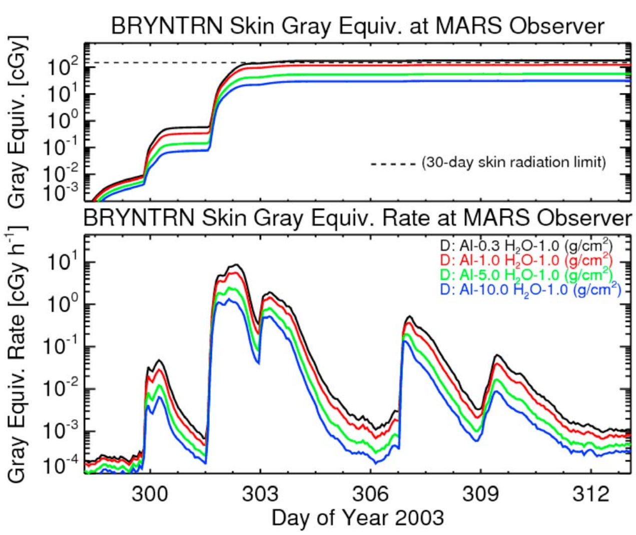

Figure 8. (top) Accumulated skin gray equivalent and (bottom) skin gray equivalent rates near Mars during the 26 October 2003 Halloween events. The aluminum (Al) and water (H_2O) depths in g cm^{-2} are displayed in the legend in the bottom plot. Note that the skin dose is above the 30 day limit of 150 cGy equivalent for the thinnest aluminum shielding areal density.

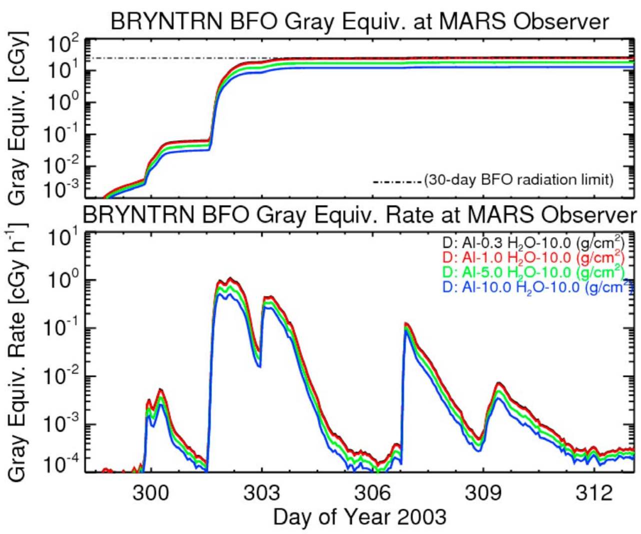

Figure 10. (top) Accumulated BFO gray equivalent and (bottom) BFO gray equivalent rates near Mars during the 26 October 2003 Halloween events. The aluminum (Al) and water (H_2O) depths in g cm^{-2} are displayed in the legend in the bottom plot. Also displayed are the 30 day BFO dose limits (25 cGy equivalent), which are exceeded for the two thinnest aluminum shields.

Earth estimates by *Parsons and Townsend* [2000] out to 1.4 AU using the radial scaling factors for the October 2003 event, as presented by Kozarev et al. (submitted manuscript, 2010).

[23] In this section the peak gray equivalent rates and accumulated gray equivalents in centigray equivalent for skin and BFO for Earth and Mars observers for the October 2003 are compared with the August 1972 peak gray equivalent rates for an aluminum shielding depth of 1 g/cm^2. This comparison is made in order to give a perspective on the severity of the 2003 event compared to one of the highest exposure events of the human space era. Since the exposures for the August 1972 event presented by *Parsons and Townsend* [2000] were only estimated for 1 AU, we will use the scaling factors obtained from EPREM (Kozarev et al., submitted manuscript, 2010) for

Table 2. Extrapolated Peak Dose Rates Behind 1 g/cm^2 Aluminum Shielding for the Skin and Bone Marrow in cGy Equivalent Per Hour for the August 1972 Event at Mars Compared to the Estimated Peak Dose Rates From This Work for the October 2003 Event

	Earth (1 AU)		Mars (1.4 AU)	
Event	Skin (cGy-Eq/h)	Marrow (cGy-Eq/h)	Skin (cGy-Eq/h)	Marrow (cGy-Eq/h)
Oct 2003	20	5	5.5	1.7
Aug 1972	207	12.8	57	4.5

Table 3. Extrapolated Cumulative Doses Behind 1 g/cm^2 Aluminum Shielding for the Skin and Bone Marrow in cGy Equivalent for the August 1972 Event at Mars Compared to the Estimated Cumulative Doses From This Work for the October 2003 Event

	Earth (1 AU)		Mars (1.4 AU)	
Event	Skin (cGy-Eq)	Marrow (cGy-Eq)	Skin (cGy-Eq)	Marrow (cGy-Eq)
Oct 2003	364	73.6	168.5	39.1
Aug 1972	2250	120	1041	63.7

the October 2003 event to extrapolate the estimated peak dose rates and cumulative doses from *Parsons and Townsend* [2000] for the 1972 event from 1 AU out to a Mars observer using

$$\dot{D}\,(Mars) = \dot{D}\,(Earth) \times (1.4)^{-X} \tag{3}$$

where $\dot{D}$ represents the peak dose rates (in cGy equivalent per hour) or the cumulative doses (in cGy equivalent) as appropriate, and X represents the numerical radial gradient factors from Kozarev et al. (submitted manuscript, 2010). The peak skin dose rate radial gradient scaling factor is X = 3.83 behind 1 g/cm^2. The cumulative skin dose radial gradient scaling factor is X = 2.29. For the bone marrow, the peak dose rate radial gradient scale factor is X = 3.14 behind 1 g/cm^2 and the bone marrow dose radial gradient scaling factor is X = 1.88. Using R = 1.4 AU for the Mars observer, the estimated peak dose rates for the August 1972 event at Mars behind 1 g/cm^2 are displayed in Table 2. The cumulative doses are displayed in Table 3. Note that the dose and dose rate values taken from *Parsons and Townsend* [2000] have been multiplied by 1.5 to convert them from cGy to cGy equivalent.

[24] From Table 2 the ratio of the August 1972 to October 2003 peak gray equivalent rate for skin and bone marrow for the Earth observer are 10.4 and 2.6 for the aluminum shielding depth of 1 g/cm^2. The ratio of the peak gray equivalent rates for skin and bone marrow for the Mars observer, 10.4 and 2.6, are again nearly identical to those for the Earth observer for the aluminum shielding depths of 1 g/cm^2. Clearly the peak dose rates from the August 1972 event appear to be much larger than those from the October 2003 event at both locations. Table 3 displays the cumulative dose calculations for both events at both locations. Note that the skin and bone marrow doses are much larger for the August 1972 event than for the October 2003 event.

[25] In the case of the 2003 event, the relative locations of the event on the solar disk were within ~20 degrees of heliolongitude for both Earth and Mars observers. For the 1972 event, the relative locations of the event on the solar disk were separated by ~155 degrees for the two observers. Hence, the estimates of cumulative doses and peak dose rates for Mars from the 1972 event, based

upon extrapolating using the radial gradients for the 2003 event, may be overestimates. However, as mentioned previously in this section, determining whether or not this is the case is not possible with EMMREM due to the poor quality of spectral data for the 1972 event at high energies.

6. Conclusions

[26] The EMMREM module is capable of characterizing the time dependent radiation environments at various locations in the solar system, and is capable of performing calculations in the Earth, Moon, Mars, and interplanetary space environment for any SEP historical event with reasonable results. Results for observers at the Earth/Moon and Mars for the 26 October 2003 SEP event, the so-called Halloween event, are presented as an example. A comparative analysis of the August 1972 event to the Halloween event suggests that cumulative doses and peak dose rates for both Earth/Moon and Mars observers significantly larger for the 1972 event.

[27] **Acknowledgments.** Research support from the NASA LWS EMMREM project and NASA grant NNX07AC14G is gratefully acknowledged.

References

Bier, S. G., L. W. Townsend, and W. L. Maxson (1998), New equivalent sphere approximation for BFO dose estimation: Solar particle events, *Adv. Space Res.*, *21*(12), 1777, doi:10.1016/S0273-1177(98)00065-9.

Billings, M. P., and W. R. Yucker (1973), The computerized anatomical man (CAM) model, *NASA Contract. Rep.*, *CR-134043*.

Hatcher, R., L. W. Townsend, N. A. Schwadron, and K. Kozarev (2009), Status of developing a near real-time capability for estimating space radiation exposure using EMMREM, paper presented at 39th International Conference on Environmental Systems, ORBITEC, Savannah, Ga., 12–16 July.

International Commission on Radiation Units and Measurements (ICRU) (1993), Quantities and units in radiation protection dosimetry, *Rep. 51*, Bethesda, Md.

International Commission on Radiological Protection (ICRP) (1991), 1990 recommendations of the International Commission on Radiological Protection, *Rep. 60*, Ottawa.

Lin, Z. W. (2009), Can the equivalent-sphere model approximate organ doses in space radiation environments?, *Nucl. Technol.*, *166*(3), 273.

NASA (2007), NASA Space Flight Human System Standard, vol. 1, Crew Health, NASA-STD-3001, Washington, D. C.

National Council on Radiation Protection and Measurements (2000), Radiation protection guidance for activities in low-Earth orbit, *Rep. 132*, Bethesda, Md.

Parsons, J. L., and L. W. Townsend (2000), Interplanetary crew dose rates for August 1972 solar particle event, *Radiat. Res.*, *153*, 729, doi:10.1667/0033-7587(2000)153[0729:ICDRFT]2.0.CO;2.

Schwadron, N. A., et al. (2006), Earth-Moon-Mars Radiation Environment Module (EMMREM), paper presented at Aerospace Conference, Inst. of Electr. and Electr. Eng., Big Sky, Mont.

Schwadron, N. A., et al. (2010), Earth-Moon-Mars Radiation Environment Module framework, *Space Weather*, *8*, S00E02, doi:10.1029/2009SW000523.

Townsend, L. W., and E. N. Zapp (1999), Dose uncertainties for large solar particle events: Input spectra variability and human geometry approximations, *Radiat. Meas.*, *30*, 337, doi:10.1016/S1350-4487(99)00060-8.

Wilson, J. W., L. W. Townsend, S. Y. Chun, W. W. Buck, F. Khan, and F. A. Cucinotta (1988), BRYNTRN: A baryon transport computer code, *NASA Tech. Memo.*, *NASA-TM-4037*.

Wilson, J. W., L. W. Townsend, W. Schimmerling, G. S. Khandelwal, F. Khan, J. E. Nealy, F. A. Cucinotta, L. C. Simonsen, J. L. Shinn, and J. W. Norbury (1991), Transport methods and interactions for space radiations, *NASA-RP-1257*, NASA, Washington, D. C.

M. A. Dayeh and M. I. Desai, Southwest Research Institute, San Antonio, TX 78238, USA.

K. Kozarev and N. A. Schwadron, Department of Astronomy, Boston University, Boston, MA 01760, USA.

M. PourArsalan and L. W. Townsend, Department of Nuclear Engineering, University of Tennessee, Knoxville, TN 37996, USA. (ltownsen@tennessee.edu)